

# Linear viscoelasticity and structure of polypropylene–montmorillonite nanocomposites

C.O. Rohlmann, M.D. Failla, L.M. Quinzani\*

*Planta Piloto de Ingeniería Química, UNS/CONICET, C.C 717-(8000) Bahía Blanca, Argentina*

Received 17 July 2006; received in revised form 18 August 2006; accepted 18 August 2006

Available online 26 September 2006

## Abstract

Polypropylene (PP)/clay composites were prepared by melt mixing in a thermoplastic mixer using a polypropylene grafted with maleic anhydride (PPg) as the compatibilizer. Concentrations of an organophilic montmorillonite (MMT) between 2 and 15 wt% and concentration ratios of PPg/clay between 1:3 and 3:1 were employed to investigate the relationship between the structural characteristics of the hybrids and their rheological properties. The structure was analyzed with electron microscopy, X-ray diffraction and melt rheology. Thermogravimetric analysis and infrared spectroscopy were also used. The clay interlayer spacing increases after mixing with PP while the addition of PPg only facilitates the partial exfoliation of the clay platelets without changing that spacing. When clay loadings of 8 wt% or larger were used, an important fraction of the original clay particles was found to remain unmodified. The dynamic moduli show little effect of the presence of the inorganic material when no compatibilizer is added or the amount of PPg or clay is too small. As the extent of exfoliation increases, the linear viscoelastic behavior of the composites gradually changes with time while in the molten state, mainly at low frequencies. Evidence of solid-like behavior appears as the concentration of clay increases, for a given PPg/clay or PP/PPg concentration, or as the PPg concentration increases (for a given clay concentration). The concentrations of PPg and clay that induce percolation were observed to have an inverse relation. Evidence of regions with large concentration of MMT was obtained in the annealed samples of composites with solid-like rheological behavior. Additionally, infrared spectra of these materials suggest the simultaneous occurrence of chemical reactions between the PPg and the surfactant or products derived from its thermal decomposition during the annealing process.

© 2006 Elsevier Ltd. All rights reserved.

*Keywords:* Nanocomposites; Polypropylene; Montmorillonite

## 1. Introduction

Polypropylene (PP) is one of the most widely used polyolefin polymers. This polymer and its blends and composites find wide application in automotive parts, extruded profiles, cable insulation, footwear, packaging industry, etc. [1]. The dispersion of organically modified layered silicates (organoclay) in PP induces enhancement in mechanical properties, flame resistance and barrier properties, compared with the pure polymer. Furthermore, these improvements are achieved for clay loadings as low as 5 wt% [2,3].

The development of polymer–clay nanocomposites (PNCs) is one of the latest evolutionary steps of the polymer technology. Different polymer–clay nanocomposites have been successfully prepared based on polymeric materials such as polyamide, epoxy, polyimide, polyurethane and polystyrene. The methods most frequently used to synthesize PNCs are three: intercalation of a suitable monomer in the clay followed by in situ polymerization, polymer intercalation from solution, and direct polymer melt intercalation using a polymer mixer or extruder [4,5]. Melt intercalation was first demonstrated by Giannelis in 1993 [6] and, since then, it has become a main stream for the preparation of PNCs. This method has the important advantage over the other two that it can be applied to large amounts of polymer in post-reactor stages.

\* Corresponding author. Tel.: +54 291 4861700; fax: +54 291 4861600.

E-mail address: [lquinzani@plapiqui.edu.ar](mailto:lquinzani@plapiqui.edu.ar) (L.M. Quinzani).

One of the most common nanoscopic fillers of PNCs is derived from the montmorillonite (MMT). MMT is a silicate with large surface-to-volume ratio (80–300 m<sup>2</sup>/g) that exists naturally in a tactoid structure comprised of several tens of stacked layers. These layers have a typical lateral dimension of 0.1–0.5 μm and layer thickness and interlayer spacing of about 1 nm. The sum of a layer and an interlayer represents the repeat unit of the stacked material, called *d*-spacing or basal spacing (*d*<sub>001</sub>). Dispersal of the nanolayers of the MMT in the polymeric matrix produces an exfoliated PNC. If the polymer molecules infiltrate the interlayer spacing preserving the stacked structure, an intercalated PNC is obtained. Although both these structures often coexist in the polymer matrix, it is believed that the outstanding properties of PNCs are derived from the large aspect ratio of the exfoliated nanolayers [2,3,5].

To facilitate the exfoliation and dispersion of the clay layers in the PP, the chemical incompatibility between the polymer and the clay has to be overcome. This is accomplished by modifying the hydrophilic nature of the clay surface and by replacing the small interlayer inorganic cations with short-chain organic cations such as alkylammonium ions [2,7]. Additionally, in the case of PNCs based on PP, a functionalized polymer such as PP grafted with maleic anhydride (PPg) must be added to enhance the filler–matrix compatibility [2,3,5]. Previous works have established the importance of having a significant level of polar functionality in the PPg that can interact with the silicate structure. These works have also established that the observed enhancement of the PP properties depends on the molecular weight and grafting degree of the PPg and on the relative concentration PPg/clay [8–13]. It has been demonstrated that the higher the value of the molar ratio of functional groups to compatibilizer chains, the lower the concentration of compatibilizer that is required for significant exfoliation [10]. Furthermore, it has been observed that if the degree of functionalization of the PPg is large, a given amount of PPg may lead to phase separation of the compatibilizer from the PP and a decrease in the degree of exfoliation [8]. Another important factor that affects the degree of exfoliation and dispersion of clay platelets is the intensity of the effective deformation applied during the mixing process. The increase of the shear in the melt decreases the size of the micron-size agglomerates but it has a negative effect on the length and aspect ratio of the tactoids [14]. With respect to the effect of the molecular weight of the PP, some authors have observed that the degree of exfoliation increases when the molecular weight of PP decreases [9,15].

Rheometry has proven to be a very powerful tool to study the microstructures of the nanocomposites. The rheological properties of particulate suspensions are sensitive to the structure, particle size, shape, and surface characteristic of the phase dispersed. In the case of clay composites, neither the presence of clay particles nor the penetration of polymer molecules between the layers of stacked clay platelets affects significantly the rheological response of the polymer. However, previous works have reported that molten PNCs exhibit a solid-like behavior at low frequencies under small-amplitude

oscillatory shear flow and have used this behavior as an indirect measure for the extent of delamination and dispersion of the silicate layers in the polymeric matrix [5]. In the case of PP nanocomposites, the large increase of the elastic modulus at low frequencies in small-amplitude oscillatory shear flow has been found to depend on the concentration of clay, type of organic surfactant used in the modification of the clay and its concentration, amount and type of compatibilizer, and deformation history applied to the PNC sample [10,12,16,17]. All these factors affect the concentration of exfoliated clay platelets. Although less noticeably, similar changes in the viscous modulus have been detected. The time-scale of the observed solid-behavior is of the order of 1000 s and it has been associated with a percolating network formed as a result of physical interaction between clay tactoids [17,18]. Ren and coworkers [18] investigated the viscoelastic behavior of a series of layered-silicate PNCs based on a model polystyrene (PS) and a model copolymer of polystyrene and polyisoprene (PS-PI). The results presented in this work show that the hybrids with silicate loadings of 6.7 wt% or larger exhibit solid-like behavior at low frequencies (the elastic modulus larger than the viscous one). In this frequency range, the dynamic moduli of the PNCs with 3.5 wt% silicate are very similar and the material with 2.1 wt% loading present liquid-like viscoelastic behavior. The authors conclude that, beyond a critical volume fraction, the tactoids and exfoliated silicate layers are incapable of freely rotating, and physical jamming or percolation occurs when the materials are subjected to small-amplitude shear flow. Galgali et al. [17] investigated the creep behavior of PP/PPg/MMT nanocomposite melts with 1:1 ratio of clay and PPg and found that the materials present a Newtonian response with very high viscosity at low strain rates and that the value of the viscosity drops fast and considerably when the shear stress increases. It was concluded that the microstructure of the dispersed platelets undergoes flow-induced orientation above the yield point, which breaks down the percolation network structure and decreases the resistance to flow. Solid-like creep behavior was observed when clay loading of 6 wt% or larger was used. Solomon and coworkers [16] have analyzed the response of PP/PPg/MMT composites (with a weight ratio of PPg to organophilic clay of 3:1) in start-up shear flow with different rest times before flow reversal. The transient reversal stress response exhibits a stress overshoot whose magnitude increases with annealing time. The transient stresses in annealed samples scale linearly with clay loading and applied strain. Based on these observations, it was suggested that microstructural changes take place during the resting time of the PNC and that the reforming of the structure in quiescent conditions after rupture is due to attractive interactions and not due to Brownian motion. The dynamic moduli were found to be sensitive to the chemistry of the surfactant used to modify the clay. The authors conclude that the prepared nanocomposites have an anisometric, non-Brownian structure and that these anisometric particulate domains are mesoscopic and contain multiple ordered platelets.

In the present article we have used small-oscillatory shear flow combined with electron microscopy, infrared spectroscopy

and X-ray diffraction techniques to study a series of PNCs based on PP, PPg and a commercial organophilic MMT. The effect that the thermo-mechanical history applied to the polymeric samples at the rheometer has on the morphology, phase stability and linear viscoelastic behavior of the PNCs has been analyzed.

## 2. Experimental

### 2.1. Materials

An isotactic PP from *Petroquímica Cuyo S.A.I.C.* ( $M_w = 330,000$  g/mol and  $M_w/M_n = 4.7$ ) and a PPg from *Uniroyal Chemical Co.* (*Polybond 3200*,  $M_w = 120,000$  g/mol,  $M_w/M_n = 2.6$ , 1 wt% of maleic anhydride) are used in this study. The clay is a commercial organophilic MMT (*Nanomer I.44P* from *Nanocor*) which has been modified with dimethyl-dialkyl ammonium halide. A thermogravimetric analysis performed on the clay shows that it contains 26 wt% of organic material and that the loss of weight begins at 220 °C (by the time the temperature reaches 275 °C, the clay has lost 5% of its original weight). This analysis was done using a *TGS-2 Perkin Elmer* system by heating the samples from room temperature to 700 °C at a rate of 10 °C/min using nitrogen atmosphere. According to optical microscopic observations (*Karl Zeiss Pol-III* equipped with a *JVC* video camera), the original clay comes in aggregates of up to 30  $\mu\text{m}$  in size.

### 2.2. Procedure of preparation of PNCs

The composites were obtained by melt mixing the polymers with the clay for 15 min in a *Brabender Plastograph* at a nominal temperature of 185 °C under nitrogen atmosphere. Polymer mix (35 g) was prepared per batch using cam-blades rotating at 50 rpm. The mixed material was removed from the mixer chamber with a spatula and compressed between aluminum plates to obtain approximately 3 mm thick samples that go from light amber to light ochre as the concentration of clay increases. In the literature, mixing times between 8 and 50 min and rotating speeds between 40 and 150 rpm have been used in different laboratory polymer mixers [9–12,16]. Some authors have also studied the effect of the operation conditions using screw extruders [12,19].

Concentrations of clay in the range from 2 to 15 wt% are considered in this study, which represent a range of 1.5–11 wt% of inorganic material. Table 1 displays the composition of the analyzed PNCs. The samples are identified with the code PC#-yz where # corresponds to the concentration of clay, and yz to the relation of PPg (y) to clay (z) weight.

### 2.3. Characterization

#### 2.3.1. Structural characterization

X-ray diffraction (XRD) was used to analyze the structure of the materials and to determine the interlayer spacing between stacked clay platelets. The study was done using a *Phillips PW1710* X-ray diffractometer equipped with a  $\text{Cu K}\alpha$  radiation source of wavelength 1.54 Å operated at 45 kV

Table 1  
Composition of the PNCs and interlayer spacing determined by X-ray diffraction

Composite	PP (wt%)	PPg (wt%)	Clay (wt%)	PPg/clay	$d_{001}$ (nm)	$d_{002}$ (nm)
MMT	—	—	—	—	2.6	1.3
PC2-11	96.3	1.7	2	1:1.2	3.3	1.3
PC2-31	92	6	2	3:1	3.3	1.4
PC5-0	95	0	5	—	3.1	1.4
PC5-13	93.3	1.7	5	1:3	3.1	1.3
PC5-11	90	5	5	1:1	3.1	1.3
PC5-21	85	10	5	2:1	3.2	1.4
PC5-31	80	15	5	3:1	3.3	1.3
PC8-15	90.4	1.6	8	1:5	2.9	1.3
PC8-11	84	8	8	1:1	2.8	1.3
PC8-31	68	24	8	3:1	2.9	1.3
PC12-18	86.5	1.5	12	1:8	2.8	1.3
PC12-31	52	36	12	3:1	2.5	1.3
PC15-31	40	45	15	3:1	2.7	1.3

and 30 mA. The diffraction spectra were recorded in the reflection mode over a  $2\theta$  range of 2–45° in steps of 0.035° using a rate of 4°/min. The original clay powder and 3 mm thick polymeric samples obtained from the melt mixing process were characterized with this technique. The PNC samples were previously slightly compress-molded at 180 °C for 3 min to produce smooth and flat surfaces.

Transmission electron microscopy (TEM), scanning electron microscopy (SEM) and optical microscopy were used to obtain complementary information of the structure of the clay and the composites at microscopic and mesoscopic levels. XRD and the above mentioned microscopy techniques have important limitations related to sample preparation and area of investigation although associated they produce very useful information. Optical microscopic observations were carried out only to check the presence of clay agglomerates in the polymeric matrix. The transmission electron microscope (*Jeol-100CX*) used in this study was operated at 120 kV. The samples of PNCs observed with this technique were ~50 nm thick slices that were cut with a *Leica UCT EM-FCS* ultra-microtome equipped with a diamond knife. The sliced sections were mounted on a 200-mesh copper grid. The smooth surfaces produced in the polymeric samples after being used in the ultra-microtome were used for scanning electron microscopic (SEM) observations. The scanning electron microscope used is *LEO EVO-40 XVP* equipment operated at 15 kV.

#### 2.3.2. Rheological characterization

The dynamic moduli of all the polymers were measured in a rotational rheometer (*Rheometrics RDAII*) using small-amplitude oscillatory shear flow between parallel plates under nitrogen atmosphere. The elastic modulus ( $G'$ ) and the viscous modulus ( $G''$ ) were obtained in a frequency range between 0.04 and 400  $\text{s}^{-1}$  and in a temperature range between 180 and 222 °C. The samples used in the rheometer were compress-molded using a hydraulic press at 180 °C for 3 min. Disks of 25 mm in diameter and 1.5 mm thick were cut from those samples. Dynamic strain sweeps were also performed on some

samples to determine the strain range of linear response of each material.

### 3. Results and discussion

The XRD patterns of the original clay and some of the PNCs are included in Figs. 1 and 2, while the basal spacing of the  $d_{001}$  and  $d_{002}$  plane peaks of the clay and most of analyzed composites are listed in Table 1. Fig. 1 displays the diffractograms of the PNCs prepared with 5 wt% of clay and different PPg/clay ratios. According to these spectra, the (001) and (002) plane peaks of the MMT, which are observed at a value of  $2\theta$  of  $3.35^\circ$  (2.6 nm) and  $7^\circ$  (1.3 nm), respectively, shift to lower values when it is mixed with the PP (see results for the PC5-0). This result indicates an increase in the separation of the clay layers due to the penetration of the polymer molecules. A similar behavior was observed by Marchant and Jayaraman [10], Modesti et al. [19], Gianelli et al. [15] in equivalent composites. The most noticeable effect of the addition of PPg to the mixture with 5 wt% of MMT is the gradual reduction of the intensity of the characteristic peaks as the PPg concentration increases (see Fig. 1 and data in Table 1). As it has been already reported in the literature, this behavior can be associated to the decrease of the size of the clay particles due to partial exfoliation [10–13].

Fig. 2 displays the diffractograms of the composites containing different amounts of clay and a constant PPg/clay ratio of 3:1. The diffractograms of the composites with 2 and 5 wt% loadings are very similar but a further increase of clay loading produces a shift of the peaks towards larger angles as well as an increase in their intensities. These observations indicate that, when the clay loading is 8 wt% or larger, an important fraction of the original clay particles remains unmodified. Similarly, Ren et al. [18] observed that the position of the  $d_{001}$  peak, although it shifts to a lower value with respect to that of the clay, is not affected by the concentration of clay for clay loadings up to 9.5 wt%. This study was done using nanocomposites based on organophilic MMT and PS or PS-PI copolymer.

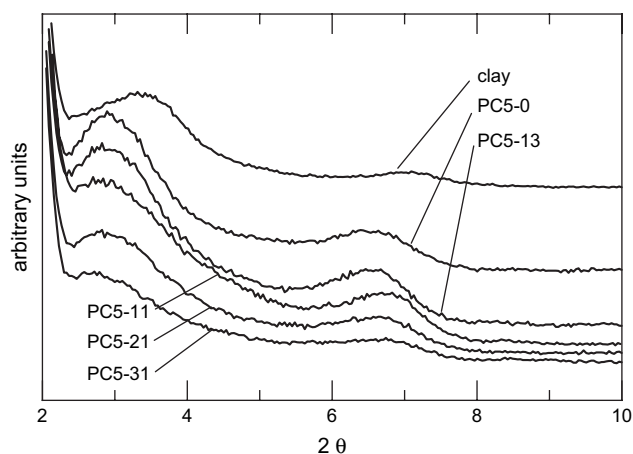


Fig. 1. XRD patterns of PP/PPg/MMT composites with 5 wt% of clay concentration and different PPg/clay ratios.

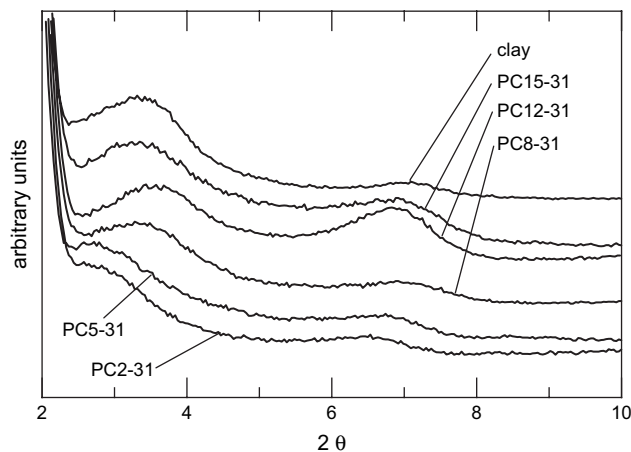


Fig. 2. XRD patterns of PP/PPg/MMT composites with 3:1 PPg/clay ratio and different clay concentrations.

The XRD results were complemented by structure analysis using TEM. Fig. 3 represents the micrographs corresponding to PC5-13 and PC5-31. The images were obtained with a magnification of  $27,000\times$ . Aggregates of clay particles having a characteristic length of about 600 nm can be appreciated in both micrographs. However, in the case of PC5-31 (Fig. 3b), a larger density of particles of different sizes is observed, in agreement with the XRD results. The exfoliation of clay platelets in PC5-31 can be better appreciated at the magnification of  $80,000\times$  (see Fig. 3c).

The morphology of the composites was also analyzed by SEM. Fig. 4 shows, as an example, a SEM micrograph of PC5-31. The displayed surface, which was obtained by an ultra-microtome cut, has been chemically treated to enhance the contrast between the clay and the polymer. The treatment consists of submerging the sample for 10 min in a solution of 0.2% v/v potassium permanganate in sulfuric acid (to slightly degrade the polymer) and then washing it several times with distilled water and 20% v/v oxygenated water [20]. A homogenous distribution of clay particles and a large dispersion of particle sizes were observed in all the materials. The larger particles have a characteristic length of about 1–2  $\mu\text{m}$ .

The results from XRD, TEM and SEM characterization confirm that the mixing technique used to prepare the composites produces the partial exfoliation of the clay platelets and that the presence of PPg as a coupling agent is important to achieve that exfoliation. Furthermore, measurement of the intensity of monochromatic light transmitted through thin films of PP, PP/PPg, PC5-0 and PC5-31 shows that the presence of the clay does not affect light transmittance.

During the rheological study, dynamic strain sweeps were performed on all the materials to find the corresponding region of linear viscoelastic behavior. This analysis pretends to avoid the use of large strains that may induce alignment of the particles of clay [18]. It was found that the linear viscoelastic region was not sensitive to the presence of PPg (in the PP/PPg blends) but it was affected by the presence of the clay. The deviation of the dynamic moduli from linear viscoelastic behavior occurs at approximately 20% in the case of PP

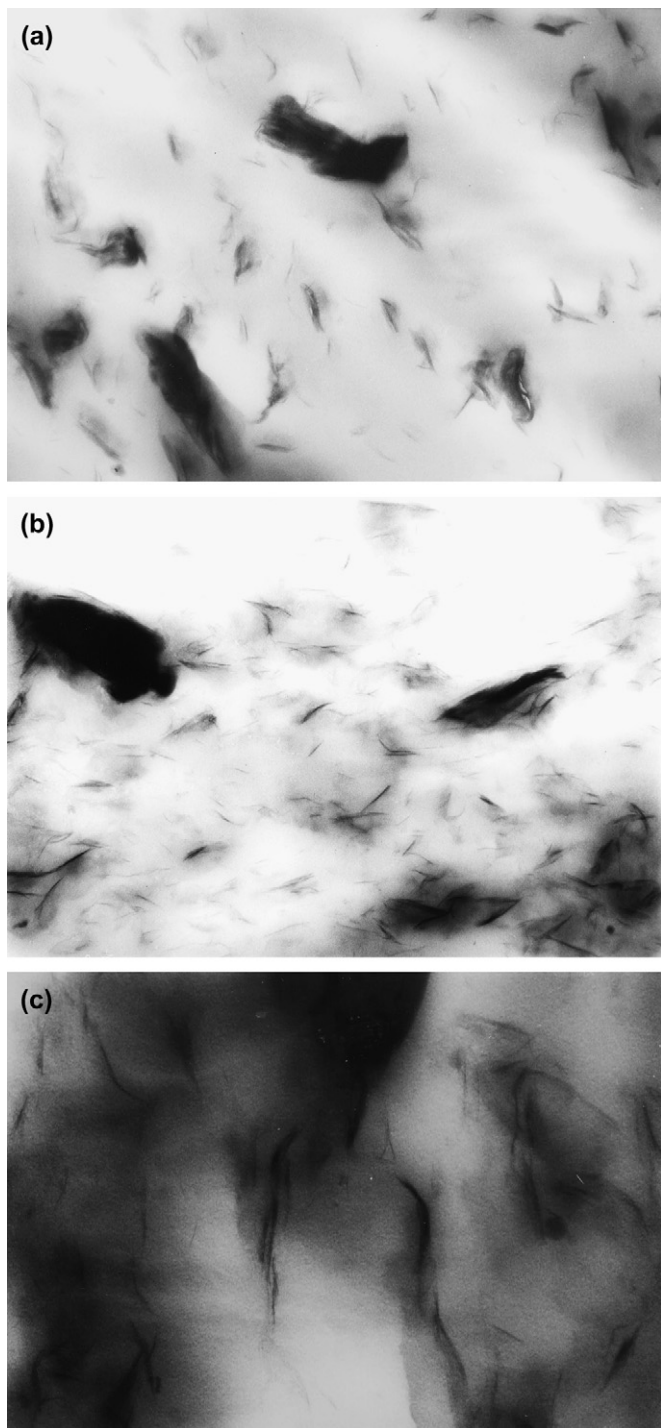


Fig. 3. TEM micrographs of PC5-13 (a) and PC5-31 (b and c). Size of the observed areas: 3255 × 2325 nm (a and b) and 1365 × 975 nm (c).

and it is reduced a factor of 2–10 by the presence of the clay (depending on the clay concentration). The reduction gets increased as the concentration of clay or PPg increases. These results indicate that the linear viscoelastic region is sensitive to the composite structure and that the increase in the amount of exfoliated platelets reduces the maximum strain of linear viscoelastic behavior. Equivalent values of strains were used by other authors [10–12].

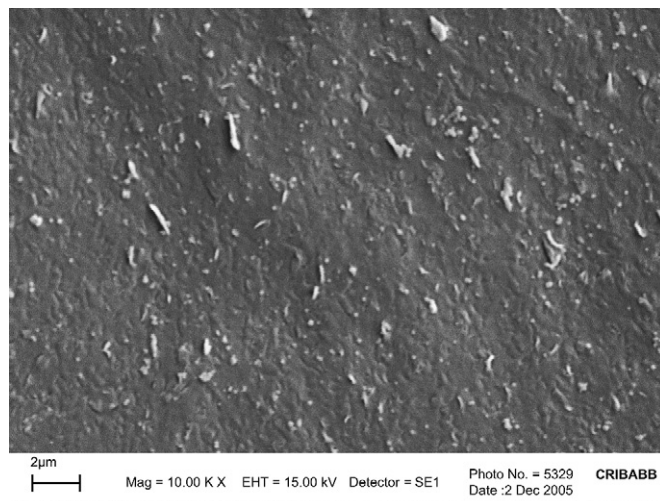


Fig. 4. SEM micrograph of PC5-31. Etching treatment was done with potassium permanganate and sulfuric acid.

Fig. 5 represents the elastic moduli of PP, PPg and the PP/PPg blends. The dynamic moduli of the homopolymers agree with the rheological behavior expected according to their molecular weight. The elastic moduli of the blends are between those of the homopolymers, although they are larger than the expected values calculated from a logarithmic mixing rule [21]. The dashed line in Fig. 5 illustrates this behavior in the case of the blend with weight concentration ratio 80:15. All the materials behave as thermo-rheologically simple polymers displaying a decrease in the dynamic parameters as the temperature increases. The time–temperature shift factors of each polymer follow an Arrhenius type of dependence with temperature. Values of 38.4 and 57.1 kJ/mol were calculated for the activation energies of PP and PPg, respectively, while

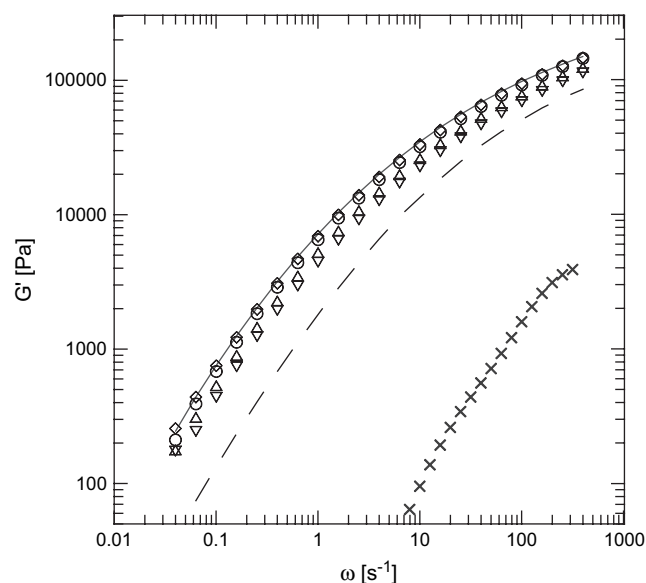


Fig. 5. Elastic modulus of PP (full line), PPg (×) and PP/PPg blends with weight concentration ratios 93.3:1.7 (◇), 90:5 (○), 85:10 (△) and 80:15 (▽) at 180 °C. Dashed line: prediction from the logarithmic mixing rule for the 80:15 PP/PPg blend.

the activation energy of the PP/PPg blends was determined to be  $39.5 \pm 2.2$  kJ/mol, which is a value very similar to that of the activation energy of PP. Galgali et al. [17] observed similar thermo-rheological behaviors.

An interesting result is the time–temperature behavior of the prepared nanocomposites. As an example of that behavior, Fig. 6a shows the dynamic moduli of PC5-31 measured during a sequence of dynamic frequency sweeps (DFS) performed at increasing temperatures on a fresh sample. At high frequencies the material presents the expected behavior with temperature, i.e. the moduli decrease as the temperature increases, although the temperature dependence is less noticeable than in the PP or the PP/PPg blends. However, at low frequencies the dynamic moduli increase as the temperature augments. This effect is more noticeable in the elastic than in the viscous modulus.  $\tan \delta$  gradually decreases approaching a value of 1 at low frequencies indicating that the material progressively changes

its behavior from liquid-like to solid-like. Considering that the moduli of the polymeric matrix decrease with temperature, the magnitude of the observed effect is even more important than it can be appreciated from Fig. 6a. The data indicate that the hybrid endures microstructural changes during the annealing conferring the material the behavior that is already accepted as distinctive of nanocomposites [5]. No effect of the annealing process was observed in the behavior of the PP or PP/PPg blends when these materials were subjected to equivalent thermo-mechanical histories than the composites.

To further analyze the effect of annealing, a sequence of selected dynamic tests was performed on a sample of PC5-31. This sequence consisted of an initial DFS at 180 °C followed by three DFS at 208 °C performed after 30, 60 and 90 min of annealing at 208 °C. Finally, the temperature was lowered back to 180 °C and a series of consecutive DFS were carried out by gradually increasing the temperature up to 208 °C. A final DFS at 180 °C was performed at the end of this sequence. Fig. 6b displays the elastic and the viscous moduli corresponding to the initial DFS at 180 °C, the sequence of tests at different temperatures after the annealing, and the final DFS at 180 °C. The data clearly show the difference that exists between the dynamic data before and after the annealing. Furthermore, the sequence of tests at different temperatures shows that the annealed material has a standard behavior with temperature, i.e., the dynamic moduli decrease as the temperature increases. Moreover, the results from the final DFS at 180 °C are practically indistinguishable from those measured at 180 °C immediately after the annealing. The annealed material presents a thermo-rheologically simple behavior and master curves of the moduli can be built with excellent agreement of the data at all frequencies. The activation energy calculated from the determined time–temperature shift factors,  $a_T$ , has a value of 38.4 kJ/mol, which agrees very well with the activation energy of the polymeric matrix. The agreement between the flow activation energies of the matrix and the hybrid indicates that the solid-like behavior of the annealed PNCs is due to the strong frictional interactions between clay layers above the percolation limit rather than confinement effects. Solomon et al. [16], Galgali et al. [17] and Ren et al. [18] already suggested this explanation.

Figs. 7–9 display the dynamic moduli of all the analyzed composites. In Fig. 7 the elastic modulus of the composites with different concentrations of MMT is presented relative to  $G'$  of the PP/PPg blend with a 93.3:1.7 ratio. This PP/PPg mix constitutes the matrix of all the composites shown in the figure and gives a PPg/clay ratio of 1:3 when 5 wt% of clay concentration is used. In Fig. 8,  $G'$  of composites with a constant clay concentration of 5 wt% and different PPg/clay ratios are shown. The data in this figure are also presented relative to the elastic moduli of the corresponding PP/PPg matrix. This way of presenting the data shows more clearly the effect of the different components on the rheological behavior. Finally, in Fig. 9 the data corresponding to composites with constant ratio 3:1 PPg/clay are displayed. Although all the materials were subjected to a series of consecutive dynamic frequency sweeps by gradually increasing the temperature

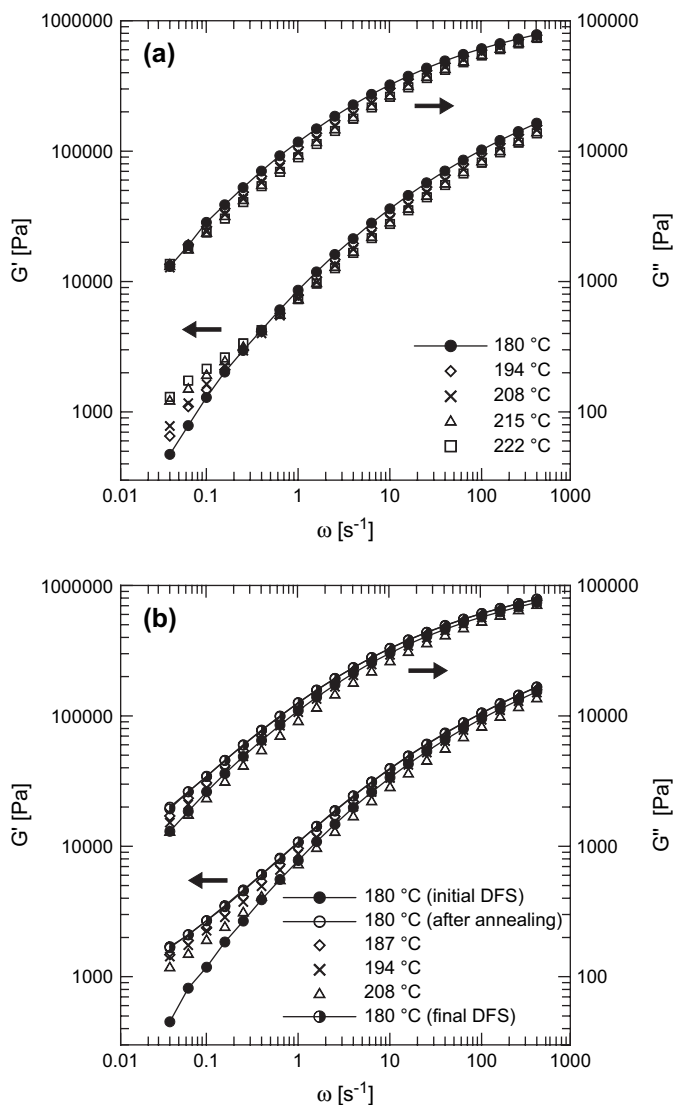


Fig. 6. Dynamic moduli of PC5-31. (a) Data corresponding to a sequence of dynamic tests performed at increasing temperatures on a fresh sample and (b) data corresponding to a sequence of dynamic tests performed at increasing temperatures on an annealed sample and data of the final test at 180 °C.

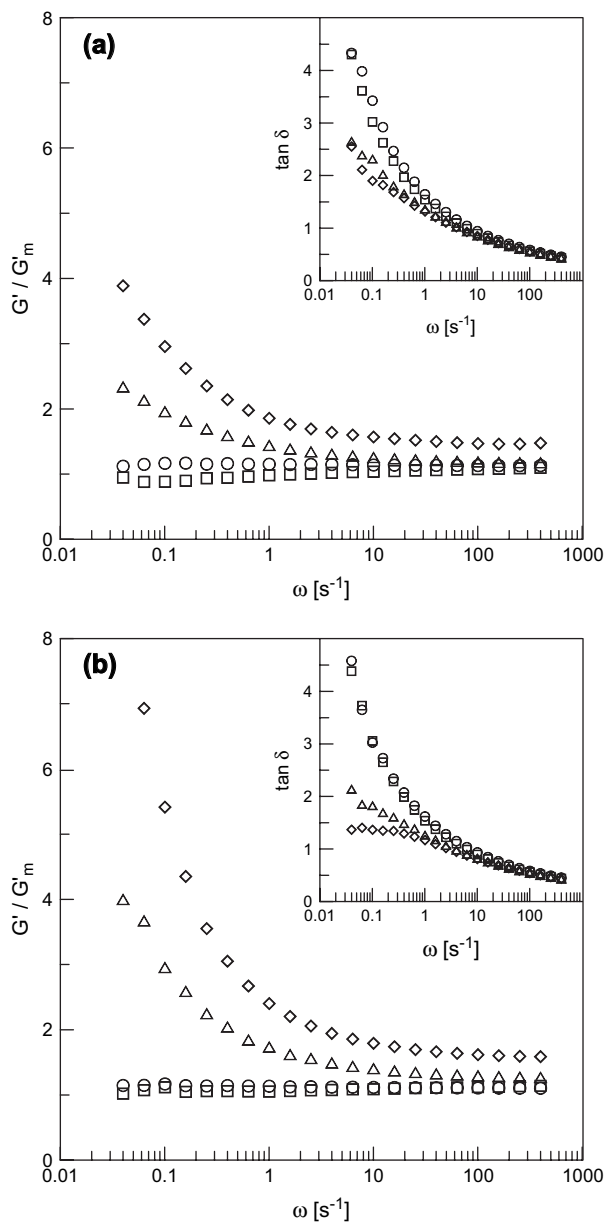


Fig. 7. Elastic modulus of PC2-11 (○), PC5-13 (□), PC8-15 (△) and PC12-18 (◇) relative to the elastic modulus of the matrix, the blend 93.3:1.7.  $\tan \delta$  data are included in the inset of figure. (a) Data from the initial DFS at 180 °C and (b) data from the final DFS at 180 °C.

from 180 to 222 °C and to a final DFS at 180 °C, only the results measured at the initial and final sweeps at 180 °C are displayed in each case. In insets of each figure, the corresponding data of  $\tan \delta = G''/G'$  are displayed.

At a given temperature, both the elastic and the viscous moduli increase when the concentration of clay increases for a constant PP/PPg ratio (Fig. 7) and for a constant PPg/clay ratio (Fig. 9). The increment of the elastic modulus is larger than the increment of the viscous one, and this effect is more noticeable at low frequencies where  $\tan \delta$  gradually decreases (see insets in figures). Moreover, in the case of PC12-31 and PC15-31,  $\tan \delta$  is smaller than 1 even for the fresh material. An increase in the dynamic moduli is also

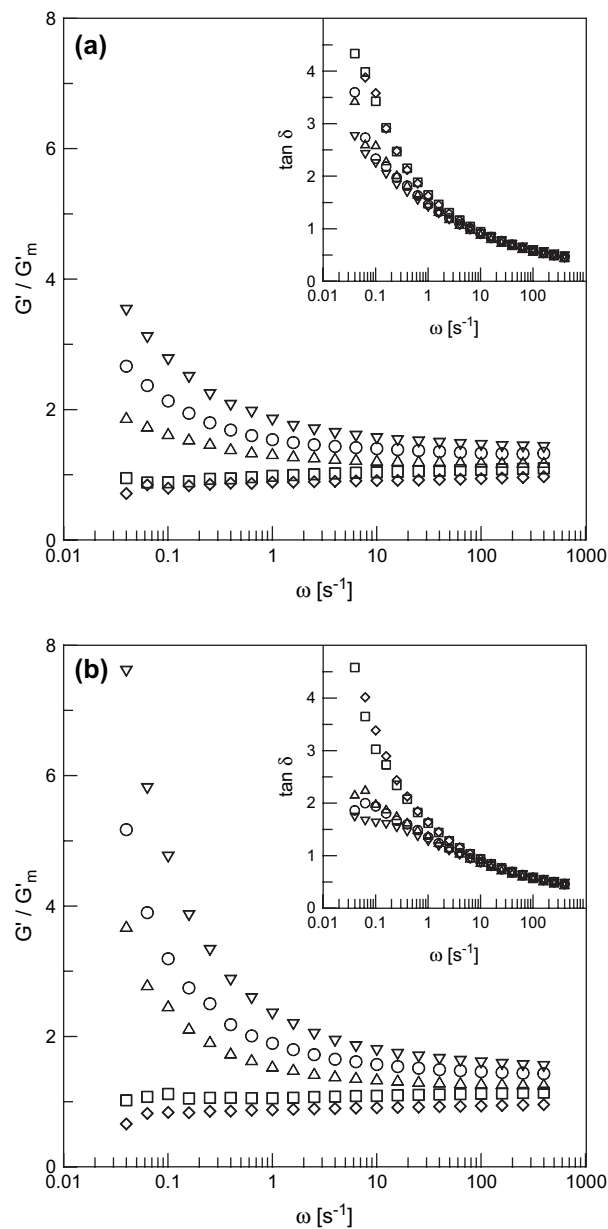


Fig. 8. Elastic modulus of PC5-0 (◇), PC5-13 (□), PC5-11 (△), PC5-21 (○) and PC5-31 (▽) relative to the elastic modulus of the corresponding PP/PPg matrix.  $\tan \delta$  data are included in the inset of figure. (a) Data from the initial DFS at 180 °C and (b) data from the final DFS at 180 °C.

observed when the concentration ratio of PPg/clay increases for a given clay concentration (Fig. 8). Practically no effect of the presence of the clay can be observed in the case of PC2-11, PC2-31, PC5-0 and PC5-13. This result demonstrates that a minimum amount of exfoliated platelets are needed to produce a visible increment in the elastic modulus of the molten composites. Furthermore, this minimum concentration of clay increases as the PPg concentration decreases, which agrees with the fact that the amount of exfoliated platelets augments when the concentration of PPg increases for a given clay concentration. No complex dependence of the dynamic moduli with clay concentration was found in this work (other than the gradual change in time while in the molten state) as

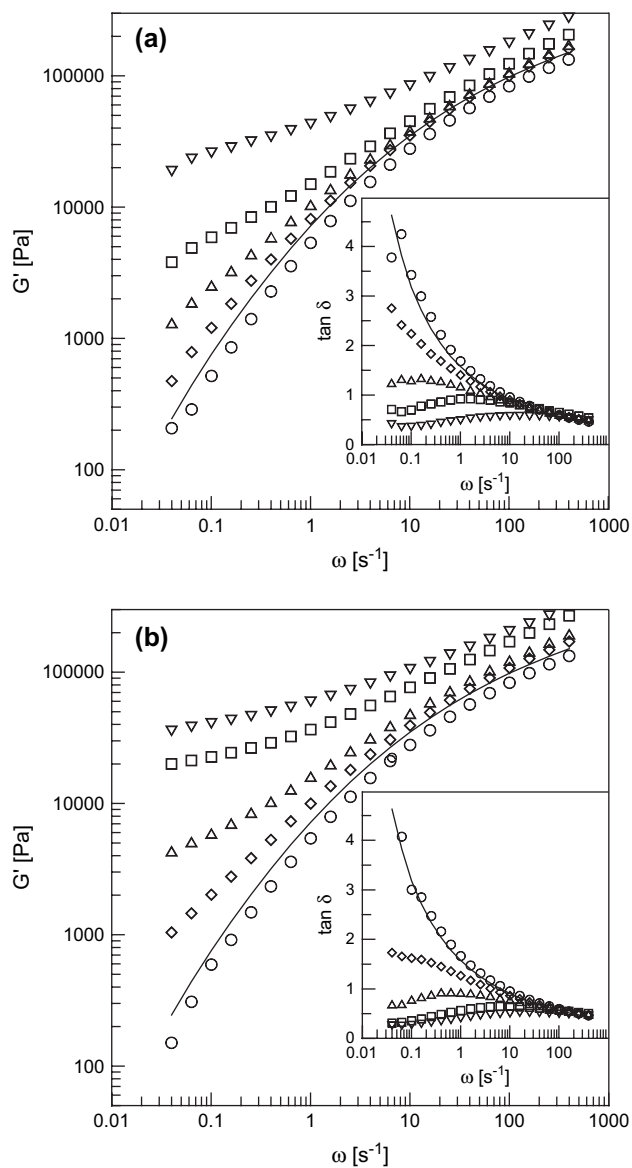


Fig. 9. Elastic modulus of PP (line), PC2-31 (O), PC5-31 ( $\diamond$ ), PC8-31 ( $\Delta$ ), PC12-31 ( $\square$ ) and PC15-31 ( $\nabla$ ).  $\tan \delta$  data are included in the inset of figure. (a) Data from the initial DFS at 180 °C and (b) data from the final DFS at 180 °C.

was reported by Solomon et al. [16] for PNCs based on PP, a PPg with 0.43 wt% of maleic anhydride and a MMT modified with stearylamine.

The comparison of the data in figures a and b shows that the annealing process induces a change in the microstructure of the hybrids. This change produces a substantial increment of the dynamic moduli (with a reduction in  $\tan \delta$ ) in all the composites except in the case of PC2-11, PC2-31, PC5-0 and PC5-13 (see Fig. 10). Moreover, the observed change in linear viscoelasticity gets larger as the clay concentration increases, for a given PPg/clay ratio, and as the PPg concentration increases, for a given clay concentration. This behavior of the composites may be explained by the development of a percolated network superstructure of individual or stacked platelets as the clay and/or PPg concentration increase. The

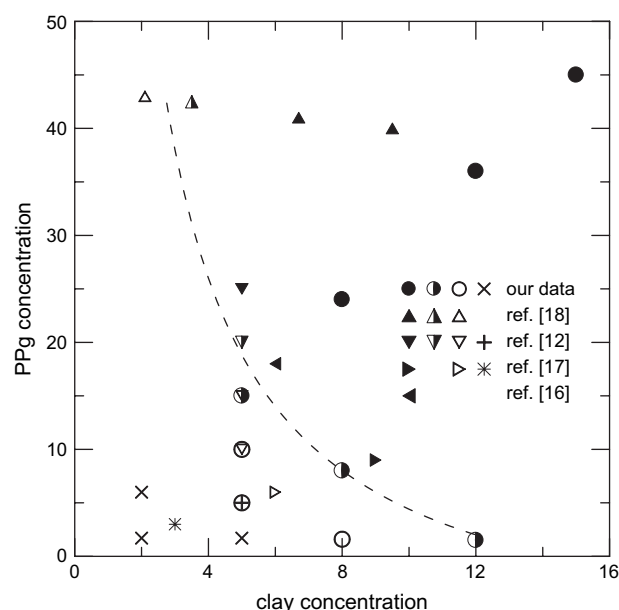


Fig. 10. Low frequency behavior of PNCs as a function of clay and PPg concentrations. Full symbols:  $\tan \delta < 1$ , half-full symbols:  $\tan \delta \approx 1$ , open symbols:  $\tan \delta > 1$  but smaller than the matrix, crosses:  $\tan \delta$  similar to the polymeric matrix.

large anisotropy of the tactoids and the individual layers prevents the free-rotation of these elements and is the cause of the relatively low value of the percolation threshold. Fig. 10 illustrates the rheological behavior observed in the different materials analyzed in this work as a function of the composition and includes the most relevant results from the literature. The full circles correspond to annealed materials that have displayed a value of  $\tan \delta$  smaller than one at low frequencies while the half-full circles distinguish the PNCs with  $\tan \delta$  very close to 1. The empty circles correspond to composites with relatively large slopes of  $G'$  and  $G''$  at low frequency (larger than those of the matrices) but  $\tan \delta$  larger than 1, and the crosses to the combinations with liquid-like behavior very similar to those of their matrices. The line was added to help in the visualization of the approximate position of the concentrations of PNCs with  $\tan \delta = 1$ . The data from Galgali et al. [17], Lertwimolnun and Vergnes [12], Ren et al. [18] and Solomon et al. [16] are included in the figure with the symbols described above and signaled with the reference number. These data correspond to PP, *Polybond 3200* and *Cloisite 6A* [17]; PP, PPg with 1 wt% of maleic anhydride and *Cloisite 20A* [12]; PS or PS-PI copolymer with 44 wt% of PS and MMT modified with dimethyldioctadecylammonium salt [18]; and PP, PPg with 0.43 wt% of maleic anhydride and MMT modified with stearylamine [16]. All these results from the linear viscoelastic behavior at low frequencies emphasize the important role played not only by the clay but also by the PPg in the formation of the hybrids. The data in Fig. 10 also highlight the inverse relation between the concentrations of clay and PPg that induce percolation. If the point of percolation of the PNC is visualized as the percolation threshold of hypothetical spheres with a diameter equal to the lateral



dimension of the platelets, an average number of platelets in each tactoid can be estimated from a simple calculation based on the fact that random spheres in three dimensions percolate at a volume fraction of 0.3 [18]. Values of 37, 24, 15 and 9 platelets can be estimated as the average number of platelets in each tactoid for clay concentrations of 12, 8, 5 and 3 wt%, respectively, using 2.6 nm as the thickness of each layer unit.

At the light of the rheological behavior observed in the PNCs, a comparative analysis of the structure of these materials before and after the annealing was done by TEM and SEM. Evidence of regions where the clay concentration seems to be larger was obtained with both these methods in the annealed samples. As an example, Fig. 11 includes two micrographs of PC5-31. Image (a) corresponds to a region of  $18 \times 13 \mu\text{m}$  observed by TEM while image (b) to a region of  $90 \times 60 \mu\text{m}$  observed by SEM. Domains with higher concentration of clay can be clearly distinguished in both photographs. These domains have a size of approximately  $18 \times 6 \mu\text{m}$  and  $50 \times 10 \mu\text{m}$ , respectively. Equivalent domains were never observed in fresh samples. This result suggests that the structural changes produced by the annealing process include the segregation of regions with large concentration of MMT.

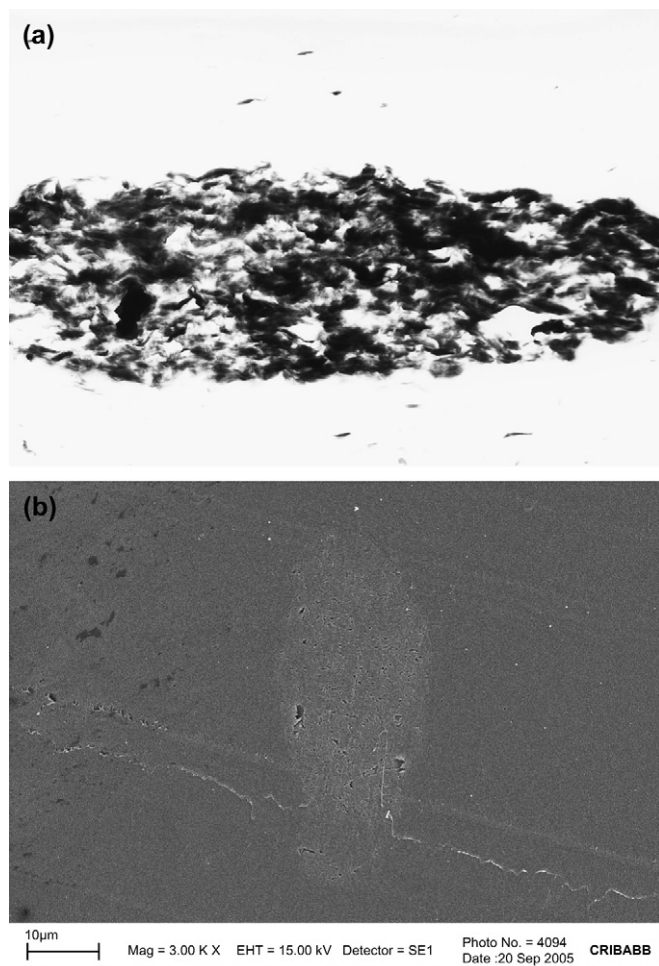


Fig. 11. TEM (a) and SEM (b) micrographs corresponding to an annealed sample of PC5-31. Size of the images:  $18 \times 13 \mu\text{m}$  (a) and  $90 \times 60 \mu\text{m}$ .

In addition to the structural changes, the annealing process produces another phenomenon, the appearance of bubbles. This phenomenon only occurs when the PPg and the modified clay are present in the composite simultaneously. The amount of detected bubbles increases when the PPg/clay ratio augments (for a given clay concentration) and when the clay concentration increases (for a given PPg/clay ratio). Very small bubbles (diameter of 500 nm or smaller) were also detected in some specimens of fresh specimens of PNCs using SEM. But those observed in the annealed samples could be appreciated with the naked eye. No mention of this phenomenon was found in the consulted literature. This observation suggests that chemical reactions may occur during the annealing process. To further analyze this possibility, samples of the processed materials were studied using FTIR spectroscopy. The comparative analysis was carried out using films prepared from fresh samples of the composites and annealed samples from the rheological tests. Fig. 12 shows the spectral region between  $1900$  and  $1500 \text{ cm}^{-1}$  for the PNCs with a 3:1 ratio of PPg/clay and different clay concentrations (PC5-31, PC8-31, PC12-31 and PC15-31) with and without annealing. To account for the differences in film thickness, the spectra were normalized with a band corresponding to PP, located at  $840 \text{ cm}^{-1}$ . Each pair of spectra that corresponds to the same type of material has been arbitrarily shifted along the y-axis for legibility reasons. Only a qualitative analysis of the spectra is possible due to the overlapping of bands and the shifting of these bands produced by the interaction between the chemical groups and the environment. The fresh samples of the polymeric nanocomposites present two bands at  $1850$  and  $1780 \text{ cm}^{-1}$  that can be ascribed to carbonyl groups of anhydride, a band at  $1770 \text{ cm}^{-1}$  and a broad band centered at  $1710 \text{ cm}^{-1}$  that result from the carbonyl groups of acids,

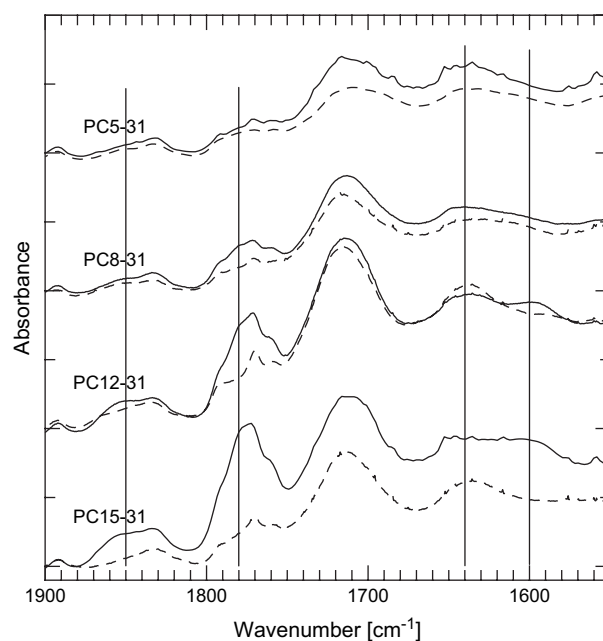


Fig. 12. Infrared spectrograms of some nanocomposites before (—) and after (---) the annealing.

amides and imides, and bands between 1680 and 1570  $\text{cm}^{-1}$  that can be associated to amides [22]. After the thermal treatment, the intensity of the absorption bands at 1850, 1780 and  $\sim 1600 \text{ cm}^{-1}$  diminishes, while the intensity of the absorption band at 1640  $\text{cm}^{-1}$  increases. These changes become less noticeable as the concentration of clay decreases for a given PPg/clay ratio. The results suggest that some of the anhydride groups of the PPg may be being consumed by reactions with substances such as the ammonium surfactant or products from its thermal decomposition that generate amides and imides. The presence of water, which may be a secondary product of this type of reactions, and/or low molecular weight products of the decomposition, may explain the formation of the observed bubbles. Similar results were found by Százdí et al. [23] from the study of the reactions between maleic grafted polypropylene and hexadecylamine.

The results from the rheological study, as well as those from the morphological structure analysis and infrared spectroscopy, suggest that both, chemical reactions between the materials used in the modification of the polymer and the clay and reorganization of the nanocomposite components with mesoscopic phase separation, are taking place during the annealing of the studied nanocomposites. Furthermore, the PP/PPg/MMT system is a thermodynamically unstable hybrid that would most likely undergo gelation and network formation during the annealing.

#### 4. Concluding remarks

We have investigated the linear viscoelastic behavior of a series of composites based on PP, maleic anhydride modified PP, and a commercial organophilic MMT. The dynamic moduli of the composites show little effect of the presence of the inorganic material when no compatibilizer is added or the amount of PPg or clay is too small (PC2-11, PC2-31, and PC5-13). As the amount of clay or PPg increases, the linear viscoelastic behavior of the PNCs gradually changes with time while in the molten state, mainly at low frequencies. Evidence of solid-like behavior appears as the concentration of clay increases, for a given PPg/clay or PP/PPg concentration, or as the PPg concentration increases (for a given clay concentration). Simultaneously, the strain range of linear viscoelasticity gets smaller. The annealed materials present thermo-rheologically simple behavior and master curves of the dynamic moduli can be built with flow activation energy very similar to that of the polymer matrix. The linear viscoelasticity of the composites emphasizes the important role played not only by the clay but also by the PPg in the formation of the hybrids. There exist an inverse relation between the

concentrations of clay and PPg that induce percolation. These results agree with observations made by DRX, TEM and SEM, which show an increasing amount the exfoliated platelets as the PPg and/or MMT concentration increases. Moreover, regions with large concentration of MMT were observed to segregate in the annealed samples of composites with solid-like rheological behavior. Additionally, infrared spectra of these materials suggest the simultaneous occurrence of chemical reactions between the PPg and the surfactant or products derived from its thermal decomposition during the annealing process.

#### Acknowledgements

The authors are grateful to the National Research Council of Argentina (CONICET), the Universidad Nacional del Sur (UNS), and the Agencia Nacional de Promoción Científica y Tecnológica (ANPCyT), for their financial support.

#### References

- [1] Karger-Kocsis J. Polypropylene blends and composites. London: Chapman and Hall; 1995.
- [2] Alexandre M, Dubois P. *Mater Sci Eng* 2000;28:1–63.
- [3] Ray SS, Okamoto M. *Prog Polym Sci* 2003;28:1539–641.
- [4] Pinnavaia TJ, Beall GW. *Polymer-clay nanocomposites*. New York: John Wiley and Sons; 2000.
- [5] Utracki LA. *Clay-containing polymeric nanocomposites*. Shawburi: Rapra Technology; 2004.
- [6] Vaia RA, Ishii H, Giannelis EP. *Chem Mater* 1993;5:1694–6.
- [7] Lee SY, Kim SJ. *J Colloid Interface Sci* 2002;248:231–8.
- [8] Kawasumi M, Hasegawa N, Kato M, Usuki A, Okada A. *Macromolecules* 1997;30:6333–8.
- [9] Kim K, Kim H, Lee J. *Polym Eng Sci* 2001;41:1963–9.
- [10] Marchant D, Jayaraman K. *Ind Eng Chem Res* 2002;41:6402–8.
- [11] Wang Y, Chen F, Li Y, Wu K. *Composites Part B* 2004;35:111–24.
- [12] Lertwimolnun W, Vergnes V. *Polymer* 2005;46:3462–71.
- [13] Perrin-Sarazin F, Ton-That M, Bureau M, Denault J. *Polymer* 2005;46:11624–34.
- [14] Vermogen A, Masenelli-Varlot K, Ségué R, Duchet-Rumeau J, Boucard S, Prele P. *Macromolecules* 2005;38:9661–9.
- [15] Gianelli W, Ferrara G, Camino G, Pellegatti G, Rosenthal J, Trombini RC. *Polymer* 2005;46:7037–46.
- [16] Solomon M, Almusallan A, Seefeldt K, Somwangthanoj A, Varadan P. *Macromolecules* 2001;34:1864–72.
- [17] Galgali G, Ramesh C, Lele A. *Macromolecules* 2001;34:852–8.
- [18] Ren J, Silva AS, Krishnamoorti R. *Macromolecules* 2000;33:3739–46.
- [19] Modesti M, Lorenzetti A, Bon D, Besco S. *Polymer* 2005;46:10237–45.
- [20] Olley RH, Hodge AM, Bassett DC. *J Polym Sci* 1979;17:627–43.
- [21] Utracki LA. *Polymer alloys and blends. Thermodynamics and rheology*. Munich: Hanser Publ; 1989.
- [22] Silverstein RM, Bassler GC, Morrill TC. *Spectrometric identification of organic compounds*. 5th ed. New York: John Wiley; 1991.
- [23] Százdí L, Pukánszky Jr B, Földes E, Pukánszky B. *Polymer* 2005;46:8001–10.